J. Agr. Sci. Tech. (2020) Vol. 22(2): 547-561

Effect of Pyrolysis Temperature and Feedstock Sources on Physicochemical Characteristics of Biochar

A. Reyhanitabar[1*], E. Farhadi[1], H. Ramezanzadeh[1], and Sh. Oustan[1]

ABSTRACT

Converting feedstock into biochar is a popular approach to overcome the disposal problem, yet the role of waste type and pyrolysis temperature on biochar properties is not understood well. In this study, biochars were produced from various feedstock such as tea waste, apple wood, wheat straw and walnut shell at 300, 400, 500 and 600°C with 1-hour residence time. The results showed that increase in pyrolysis temperature significantly decreased biochar mass yield. The maximum and minimum mass yields were observed in walnut shell at 300˚C and apple-wood-derived biochars at 600˚C by 69 and 20%, respectively. The produced biochar had pH range between 5.3 to 9.7, and its pH value and ash content increased significantly with increasing pyrolysis temperature, except for walnut shell. Total concentrations of P, Ca, K, Na, Fe, Zn, Cu, and Mn and available concentrations of K, Ca, Mg, and P increased with pyrolysis temperature increasing in all samples, except at walnut shell-derived biochar. According to CHN analysis, by increasing pyrolysis temperature, the total carbon concentration increased but total nitrogen and hydrogen concentrations decreased. The pH value decreased with time until 72 hours, beyond which a near steady-state condition was attained. Relationships between pH and $CaCO_3$-eq content of biochars were close and linear. The FT-IR spectra showed that aromatic C increased by increment in heating. Also, by increasing pyrolysis temperature, the mean pore diameter decreased but micropores volume increased and led to increase in the specific surface area of biochars. The results of this study suggest that biochars produced at 300 and 400˚C may have potential as fertilizer in calcareous soils because of low pH and EC, with high mass yield.

Keywords: CHN analysis, FT-IR spectra, Organic waste.

INTRODUCTION

Nowadays, attention to biochar as a solution for mitigating global-warming effects and low-cost applicant for organic and non-organic pollutant decontamination is gradually increasing (Beesley *et al*., 2011). In addition, biochar can be used as a soil amendment for improving biological, chemical, and physical attributes of soil (Bera *et al*., 2016 and 2019). The structural and physicochemical properties of biochars can directly regulate the intent of use alongside the final impacts (Sandhu *et al*., 2017; Zhang *et al*., 2019). The thermochemical decomposition of feedstock under highly oxygen-limiting conditions is known as pyrolysis, a common process of biochar production. Two main factors govern properties of biochars: source of feedstock (Enders *et al*., 2012; Cantrell e*t al*., 2012; Bera *et al*., 2018; O'Connor *et al*., 2018) and the pyrolysis conditions such as pyrolysis temperature, heating rate and duration (Mohan *et al*., 2006; Shen *et al*., 2019; Rens *et al*., 2018; Rostamian *et al*, 2015). Thorough acquaintance with biochar production and knowledge about pyrolysis process details and feedstock constituents is key to prediction of biochar behavior for any

[1] Department of Soil Science, Faculty of Agriculture, University of Tabriz, Tabriz, Islamic Republic of Iran.
***** Corresponding author; e-mail: areyhani@tabrizu.ac.ir

[DOR: 20.1001.1.16807073.2020.22.2.21.9]

particular application purpose. The type of feedstock is an important factor that influences biochar morphological and structural properties. Otherwise, because of the different constituents of feedstock elements, biochars are widely varied in chemical compositions (Liu *et al.*, 2018). Some characteristics of biochar such as pH, Cation Exchange Capacity (CEC), and Electrical Conductivity (EC) are affected by nature of the feedstock. In general, feedstock comprises three types of natural polymers: cellulose (50% of dry matter), hemicellulose (10-30% in woods and 20-40% in grass materials), and lignin (20-40% in woods and 10-40% in grass materials). Generally, CEC in biochar derived from woody material is lower than manure originated type (Singh *et al*., 2010). Woody biochars also have a greater volatile content than grass materials (Jindo *et al*., 2014).

Besides feedstock nature, the pyrolysis temperature has a primary role in biochars characteristics. The temperature of pyrolysis and maintenance of a specific progress to produce biochar makes great difference among final products. Changes in pyrolysis temperature from low to high due to decrease in aliphatic groups, increase in surface area, and more development in aromatic compounds has been reported (Jindo *et al*, 2014; Jia *et al.*, 2018), but reference to source of feedstock difference between surface areas could be more significant (Ghani *et al*., 2013, Luo *et al*., 2015).

The aim of this study was to compare physicochemical characteristics of biochars derived from different feedstock (agricultural wastes) through changing in pyrolysis temperature. The residuals from harvesting and pruning of tea, wheat, apple tree, and walnut are among the major agricultural wastes in Iran that are produced over thousands of tons every year (Banitalebi *et al.*, 2019; Karimi Alavijeh and Yaghmaei, 2016). Therefore, pyrolysis could be a magnificent way in management of wastes and production of useful amendments to soil to inhibit greenhouse gas emission (Mukome *et al*., 2013) and improve soil properties (Yu *et al.*, 2019). The thermochemical properties of different agricultural wastes obtained at the 300–600˚C temperature range differ. While some reports indicate pyrolysis temperature effects on biochars physicochemical properties, it seems more research is needed to complete observation of relationships between some morphological and important characteristics of biochar.

MATERIALS AND METHODS

Feedstock Pyrolysis

Initial feedstock samples included Tea (*Camellia sinensis* L.) harvesting procedure waste (TwBC), Wheat (*Triticum aestivum* L.) straw husk (WhBC), Apple (*Malus pumila*) tree wood pruning waste (ApBC), and Walnut (*Juglans regia* L.) shell waste (WsBC). These were obtained as by-product from agriculture wastes. All the feedstocks were washed by distilled water and then oven dried at 60°C for 24 hours to reduce the moisture to less than 10% w/w (Liu and Han, 2015). Dried feedstock was milled to less than 2 mm for biochar production. The sieved feedstock was placed in a ceramic covered crucible and located inside an electrical furnace under Ar gas atmosphere (5 L min^{-1} of Ar flow) was heated from room temperature to different final temperatures (300, 400, 500 and 600°C). The heating rate was 10°C min^{-1} in all treatments (slow pyrolysis) and feedstocks were kept in furnace 1-hour after reaching the final temperature. The bio-oil was negligible and by-product gases exhausted from the furnace during pyrolysis process. To inhibit oxidation reactions of biochars in contact with atmosphere, the biochars were stored at room temperature in a desiccator until all analyses were made (Yang *et al*., 2017).

Yields, Ash Content, pH and Electrical

[DOR: 20.1001.1.16807073.2020.22.2.21.9]

Conductivity (EC)

The biochar mass yield was calculated as the proportion of produced biochar to initial weight of original feedstock (105°C) before pyrolysis. The ash content was measured by combusting biochar at 750°C for 6 hours and measuring the residue after combustion according to D1762-84 (ASTM, 2007). Weighting was taken after sample cooling in a desiccator for 1 hour. The pH and EC were measured (AZ 8301, AZ instruments, Taiwan) at 1:10 ratio of biochars to distilled water after 1-hour shaking by end-to-end shaker (Li *et al*., 2013). Furthermore, to identify the pH variability versus time (pH dynamic), pH was measured in suspensions at 1, 4, 24, 48, 72 and 168 hours.

Elemental Composition

Total concentration of Carbon (C), Nitrogen (N) and Hydrogen (H) were measured by CHN analyzing on Vario EL (Elementer Co, Germany). The available concentration of Calcium (Ca), Magnesium (Mg) and potassium (K) were determined by digestion in standardized 1M HCl solution (Singh *et al*., 2017) and biochar available Phosphorus (P) by standardized 0.5M solution of $NaHCO_3$ (Singh *et al*., 2010). The total concentration of each element was measured by dry digestion method (Westerman, 1990). The concentrations of elements were determined by AAS, using Shimadzu AA-6300 instrument (Shimadzu Inc. Japan) and P by Spectrophotometer at 730 nm.

Calcium Carbonate Equivalent

A solution with 0.5 g of biochar and 10 mL of standardized 1M HCl was prepared and shaken for 2-hours by end-over-end shaker, and left for 16-hours. Then, it was titrated using standardized 0.5M NaOH solution until reaching pH~7.0. The volumes of NaOH solution consumed for sample (a) and blank solution (b) (without biochar) were recorded. The $CaCO_3$ Equivalent content (CCE) was determined as follows (Singh *et al*., 2017):

$$\%\ CaCO_3\text{-Eq} = \frac{Molarity\ of\ NaOH \times (b-a) \times 10^{-3} \times 100.09 \times 100}{2 \times mass\ of\ biochar}$$

Fourier-Transform Infrared (FT-IR) Spectroscopy

The pellet technique was employed by FT-IR spectroscopy method using a Tensor 27-FTIR (Bruker Optics, MA). To obtain pellets, 1 mg of dried biochar/feedstock was mixed with 300 mg of KBr (pre-dried, spectroscopic grade) and the spectra were obtained with 60 scans with wave numbers ranging from 400 to 4,000 cm^{-1} and resolution of 4 cm^{-1}. The following broad-band assignment was used to identify functional groups: 3,400 to 3,410 cm^{-1}, H-bonded O–H stretching vibrations of hydroxyl groups from alcohols, phenols, and organic acids; 2,850 to 2,950 cm^{-1}, C–H stretching of alkyl structures; 1,620–1,650 cm^{-1}, aromatic and olefinic CDC vibrations, CDO in amide (I), ketone, and quinone groups; 1,580 to 1,590 cm^{-1}, COO- asymmetric stretching; 1,460 cm^{-1}, C–H deformation of CH_3 group; 1,280–1,270 cm^{-1}, O–H stretching of phenolic compounds; and three bands around 460, 800, and 1,000 – 1,100 cm^{-1}, bending of Si–O stretching. All feedstocks/biochars were ground into powders prior to the spectral acquisition (Wu *et al*., 2012; Guo and Chen, 2014; Sun *et al*., 2017).

Surface Area and Morphology

Based on Brunauer, Emmet, and Teller (BET) theory, surface area and pore volumes were calculated using multi-point adsorption data. Surface morphology was measured using a BELsorp-mini (BEL Japan, Inc.). The N_2 adsorption isotherms were measured at 77 K from the 0.01–0.3 P/Po linear segment. Samples were degassed at 180°C

[DOR: 20.1001.1.16807073.2020.22.2.21.9]

for at least 24 hours under vacuum conditions prior to nitrogen adsorption at liquid nitrogen temperature (Singh *et al*., 2017). The Scanning Electron Microscopy (SEM) method was used to analyze morphology for biochars pyrolyzed at 300 and 600˚C. The MIRA3 FEG-SEM (Tescan Co, Czech) was employed with a theoretical resolution of 1 nm and an acceleration of 30 kV.

X-Ray Diffraction

X-ray diffraction was performed on the biochars using a Bruker D8 X-Ray diffractometer (Germany). Three grams of each char was granulated for powder diffraction using Cu Kα1 radiation (40 kV, 40 mA) from 5° to 60° (2θ) with 0.25 second measurement interval at 25°C.

Statistical Analysis

All of the experiments were conducted in duplicate or triplicate, and the average values were reported. Data were analyzed using the statistical package MSTAT-C (MSTAT-C, 1989). Analysis Of Variance (ANOVA) as a factorial experiment based on completely randomized design was employed to determine significant differences among treatments including type of feedstock, pyrolysis temperature and their interactions, and the means were compared by the Duncan's multiple range tests at the 1 and 5% probability level. The diagrams were drawn by the Excel software.

RESULTS AND DISCUSSION

Analysis of variance showed that the main effects of pyrolysis temperature and feedstocks and interactions between them on mass yield, ash content, pH variation, EC and CCE of biochars were significant (P≤ 0.01) (Table 1). The mean yields of the biochars decreased by increasing pyrolysis temperature from 300 to 600˚C in all feedstock (Figure 1-a). The maximum mean of yield for biochars at 300˚C was 49.6% followed by 38.7, 31.8, and 27.05% for 400, 500 and 600˚C, respectively. At low temperature, less compaction of aliphatic compounds and waste of CO_2, H_2 and CH_4 lead to the maximum mass (Amonette and Joseph, 2009; Bera *et al*., 2017). By increasing pyrolysis temperature, the yield declined owing to dehydration of hydroxyl groups and thermal decomposition of ligno-cellulose structures (Antal and Gronli, 2003). In this study, there was significant difference in mass yields and feedstocks between pyrolysis temperatures (Figure 1). The maximum mass yield belonged to WsBC at 300˚C (69.3%) and the minimum value was for ApBC at 600˚C (19.8%). There was a significant difference among treatments because of heating that led to volatile pyrolytic materials turn to organic molecules with low weight and a wide range of gases (Thangalazhy-Gopakumar *et al*.,

Table 1. Analysis of variance for mass yield, CCE, ash content, pH, and EC of the tested biochars as affected by pyrolysis temperature.[a]

	Mean of Square (MS)						
Source of variation	df	Mass yield	CCE	df	Ash content	pH	EC
Feedstock type	3	3.002**	2.299**	3	23.279**	0.132**	32.439**
Pyrolysis temperature	3	5.073**	20.554**	4	1.566**	0.332**	2.526**
Feedstock type×Pyrolysis temperature	9	0.433**	0.092**	12	0.417**	0.008**	1.432**
Error	16	0.04	0.197	20	0.004	0.00005	0.002
CV (%)		3.33	11.77		2.20	0.30	3.30

[a] Ash content, pH, and EC measured with in biochars and initial feedstocks, and df= Degree of freedom.

** Significant at P≤ 0.01.

[DOR: 20.1001.1.16807073.2020.22.2.21.9]

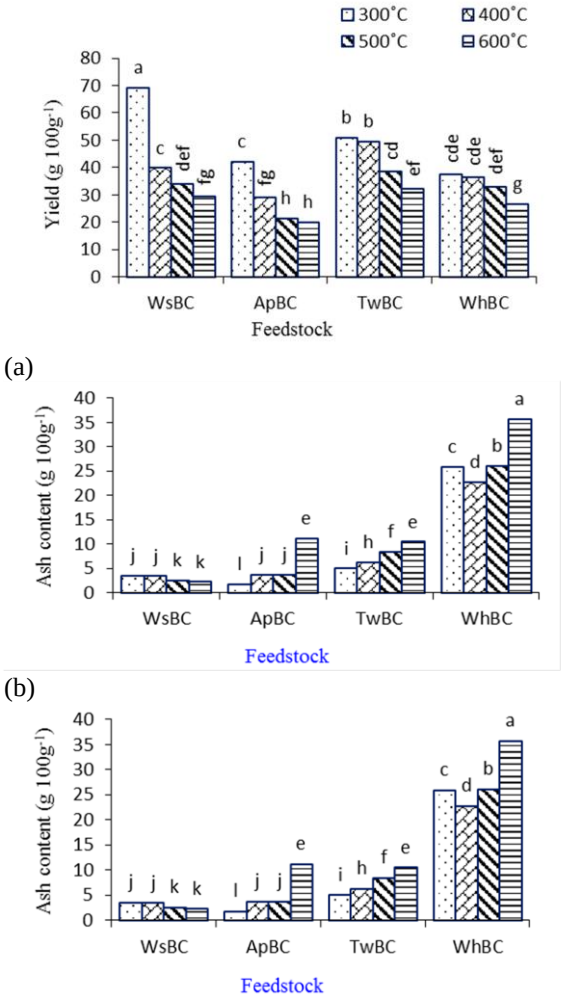

Figure 1. Interaction effects of pyrolysis temperature and feedstock on mass Yield (a), Ash content (b), and Electrical conductivity of biochars (c).

2010).

WsBC and WhBC samples had the lowest and highest ash content, respectively (Figure 1-b), which increased with pyrolysis temperature. A significant difference ($P \leq 0.05$) between pyrolysis temperatures was observed in ash content. The pyrolysis temperature of 600˚C had the highest ash content (14.8%) among other heating treatments. Singh *et al*. (2017) reported 21.2% for 550˚C and 23.8% ash content for 700˚C at the end of the wheat straw pyrolysis process. Tsai *et al*. (2012) suggested that the concentration of mineral fraction gradually increased by increasing pyrolysis temperature.

The Electrical Conductivity (EC) of biochars was higher than the original feedstocks (Figure 1-c). Generally, the EC increased with pyrolysis temperature from 300 to 600˚C. This phenomenon probably resulted from higher ash content at high pyrolysis temperature (Claoston *et al*., 2014) and loss of volatile compounds and increase in mineral fraction, especially K^+ ion in ash contents with high mobility (Kim *et al*., 2012, Joseph *et al*., 2007). In this study, there was a significant linear relation ($r= 0.97$, $P \leq 0.01$) between EC and ash content for all biochars. Also, there was a significant relation between pH and ash content in the four prepared biochars ($r= 0.56$, $P \leq 0.05$), in which correlation increased after excluding WsBC ($r= 0.72$, $P \leq 0.01$).

In this experiment, pH of biochars ranged from 5.2 to 9.7. The value of pH in WhBC was high compared to others samples and ApBC was lowest. Also, by increasing the pyrolysis temperature from 300 to 600˚C, pH of biochars turned more toward alkaline reaction. The pH measurement in biochars may be influenced by other factors like solid/ solution ratio, background solution and shaking time prior to measurement, like in soil measurements. In this study, significant differences in pH of the produced biochars were observed at the same conditions. At the carbonization process, acidic functional groups relatively decreased by rise in temperature (Reeves *et al*., 2007) and alkaline elements content enriched, which led to alkaline pH. The pH was also affected by feedstock type in the experiment. The TwBC had acidic pH resulting from dissolution of silicate containing minerals and hydroxide of Fe and Al in solution, whereas alkalinity of pH in biochar could be because of dissolved carbonate, oxides, and hydroxides functional groups. Amounts of ash play a main role in pH, however, mineral fractions was primary determinant of variations among different feedstock (Figure 2).

[DOR: 20.1001.1.16807073.2020.22.2.21.9]

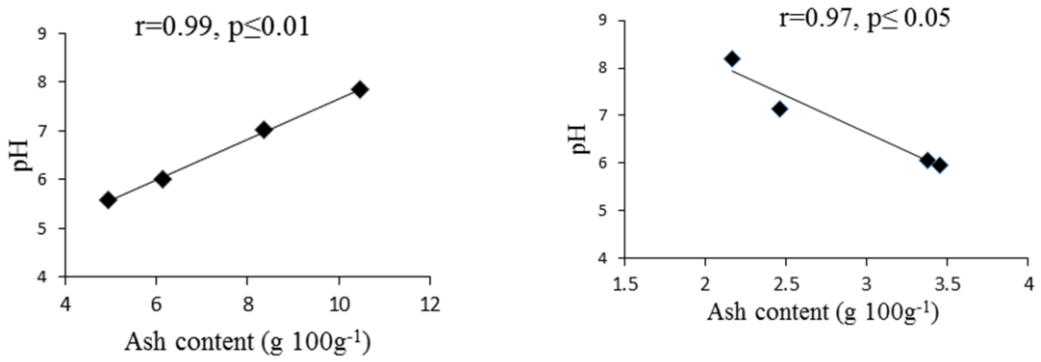

Figure 2. Relationships between ash content and pH of TwBC (left) and WsBC (right).

The CaCO3-Eq amounts (CCE) had a strong positive linear correlation (r= 0.90, P≤ 0.01) with pH (Figure 3) among all biochars. The relationship indicated the role of $CaCO_3$ on biochars pH.

The pH dynamic curves showed that pH decreased in time steps, and beyond 72 hours, a near steady-state condition was achieved as shown in Figure 4. The maximum and minimum pH variations were observed at ApBC at 300 and 600˚C by 0.8 and 0.02, respectively. Mineral fraction dissolution and carbon oxidization could affect pH values. Curves variations of temperature were fixed in biochars among incubation time, except for 300˚C. At the 300˚C, a fast decrement occurred in pH values until 72 hours, and continued similarly for other temperatures. The use of pH-dynamic curves makes it possible to predict biochar behavior by time. It can be used in management of combined fertilizers in calcareous soils to reach optimum efficiency.

Elemental analysis results are shown at Table 2. The H/C and C/N atomic ratio are major characteristics of biochars. Aromaticity of biochars could be evaluated from H/C ratio (Zhang *et al*., 2019). In this study, with increase in the pyrolysis temperature from 300 to 600˚C, H/C ratio decreased (Table 2). Sufficient transforming of material from its feedstock must possess H/C_{org}< 0.7 to be considered biochar, based on the requirement of the International Biochar Initiative (IBI, 2015). The decline in H content was a sign of dehydration reaction at high temperatures in all biochars after the H/C_{org} ratio decreased. At high temperature, depolymerization of feedstock happens, which is due to productions of lower molecular weight molecules. The highest and lowest content of H/C was observed at wheat straw feedstock at 25˚C and WhBC at 600˚C, respectively (Table 2).

According to our results, feedstock type and pyrolysis temperature significantly influenced

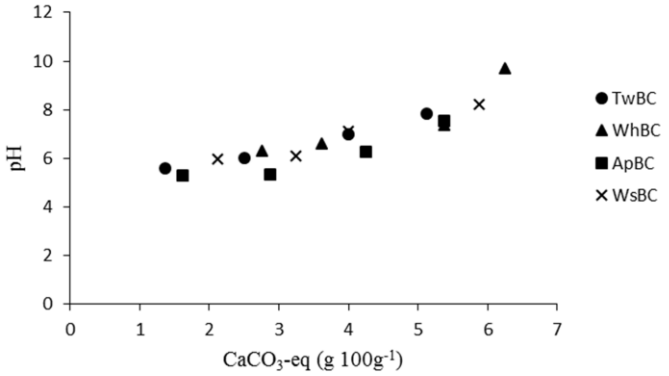

Figure 3. Relationships between pH and $CaCO_3$-eq content of biochars.

[DOR: 20.1001.1.16807073.2020.22.2.21.9]

Table 2. Elemental composition of feedstock (25°C) and produced biochars at different pyrolysis temperature.

Feedstock	Pyrolysis temperature (˚C)	Elemental composition			Atomic ratio	
		C (g 100 g^{-1})	N (g 100 g^{-1})	H (g 100 g^{-1})	H/C	C/N
TwBC	25 [a]	50.04	3.748	6.603	1.57	15.57
	300	54.57	5.481	3.370	0.74	11.61
	600	58.81	5.246	2.555	0.52	13.07
WhBC	25 [a]	39.70	1.503	6.267	1.88	30.80
	300	47.73	1.717	2.212	0.55	32.42
	600	53.62	1.692	1.252	0.28	36.96
ApBC	25 [a]	49.60	0.434	6.040	1.45	133.28
	300	62.63	0.682	3.060	0.58	107.09
	600	66.69	0.525	1.997	0.36	148.14
WsBC	25 [a]	48.06	0.708	5.655	1.40	79.16
	300	57.55	0.917	4.114	0.85	73.19
	600	81.09	0.736	2.347	0.34	128.49

[a] Initial feedstock.

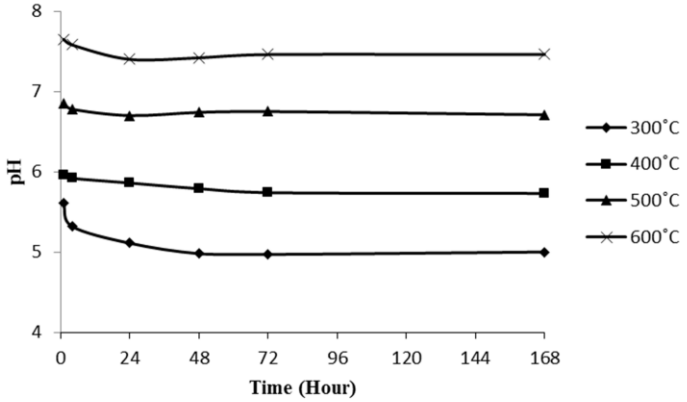

Figure 4. pH dynamic in TwBC.

the total concentration of elements (Table 3). In relation to the feedstock, the maximum concentration of total P was measured in Tea waste biochar and the highest concentration of total Ca, Mg, K and Na were measured in WhBC. For micronutrients, the highest total concentration was observed at the pyrolysis temperature of 600˚C. Concentration of the micronutrients increased by pyrolysis temperature, except in WsBC. This trend had been observed for Fe, Zn, Cu, and Mn concentration. The TwBC had a higher concentration of Zn, Cu and Mn among feedstock, whereas WhBC had more Fe. The 600˚C treatment had the maximum concentration of elements concentration (Table 3).

The correlation between available and total P concentration was not strong (Figure 5) and there was a systematic departure from linearity, (r= 0.59, P≤ 0.05, left), but by removal of the TwBC data, a close relation between available and total P was observed in biochars (r= 0.97, P≤ 0.01, right).

Results showed significant correlations between available and total concentrations of

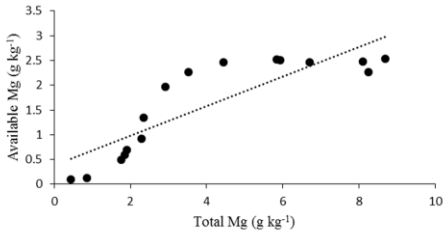

Figure 6. Relationships between available and total concentration of Mg of TwBC, WhBC, WsBC and ApBC at four pyrolysis temperatures.

[DOR: 20.1001.1.16807073.2020.22.2.21.9]

Table 1. Total and available concentration of Ca, Mg, K and P in biochars at different pyrolysis temperature.[a]

Feedstock	Temp(˚C)	Available (mg g^{-1})			Total (mg g^{-1})									
		Ca	Mg	K	P	Ca	Mg	K	P	Fe	Zn	Cu	Mn	Na
TwBC	300	5.47^{j}	1.97^{d}	2.26^{j}	0.15^{e}	21.92^{e}	2.92^{g}	3.48^{cd}	5.4^{d}	250^{f}	42.88^{c}	33.25^{de}	363.7^{c}	1.09^{bcd}
	400	7.52^{g}	2.27^{c}	3.12^{i}	0.45^{c}	25.09^{d}	3.52^{f}	6.24^{bc}	6.25^{c}	300^{f}	45.8^{c}	37.95^{c}	421.89^{c}	1.38^{abcd}
	500	13.25^{c}	2.47^{b}	4.63^{g}	0.84^{a}	26.44^{d}	4.45^{e}	10.15^{b}	6.98^{b}	390^{e}	59.59^{b}	55.21^{b}	539.44^{b}	1.53^{abc}
	600	15.62^{a}	2.5^{ab}	5.79^{f}	0.74^{b}	29.34^{bc}	5.93^{d}	11.44^{b}	7.98^{a}	430de	67.26^{a}	63.75^{a}	670.24^{a}	1.8^{ab}
WhBC	300	8.91^{f}	2.52^{a}	22.65^{c}	0.47^{c}	26.68^{d}	5.84^{d}	40.65^{b}	1.18^{h}	450^{cd}	18.05^{h}	8.71^{kl}	30.43^{h}	1.14^{bcd}
	400	9.21^{e}	2.47^{b}	23.86^{bc}	0.72^{b}	28.82^{c}	6.71^{c}	65.77^{a}	1.55^{g}	520^{bc}	23.34^{g}	8.99^{jkl}	37.18^{gh}	1.53^{abc}
	500	9.43^{d}	2.48^{b}	25.17^{b}	0.73^{b}	29.31^{bc}	8.1^{b}	72.7^{a}	1.95^{f}	570^{b}	28.66^{e}	11.2^{ij}	45.3^{gl}	1.69^{ab}
	600	9.53^{d}	2.54^{a}	34.94^{a}	0.75^{ab}	30.91^{b}	8.7^{a}	75.28^{a}	2.14^{f}	920^{a}	34.95^{d}	13.94^{h}	47^{g}	2.21^{a}
ApBC	300	3.41^{l}	0.5^{i}	1.96^{k}	0.084^{ef}	5.86^{i}	1.75^{i}	2.35^{de}	0.22^{klm}	80^{hi}	17.68^{h}	13.09^{hi}	36.54^{gh}	1.03^{bcd}
	400	5.88^{i}	0.92^{f}	3.52^{hi}	0.11^{ef}	12.48^{f}	2.3^{h}	7.77^{bc}	0.48^{j}	160^{g}	25.06^{fg}	19.21^{g}	43.45^{g}	1.26^{bcd}
	500	6.78^{h}	1.35^{e}	3.82^{h}	0.26^{d}	13.81^{f}	2.34^{h}	8.95^{b}	0.55^{j}	190^{g}	26.61^{ef}	26.46^{f}	65.86^{f}	1.27^{bcd}
	600	13.46^{b}	2.26^{c}	8.00^{d}	0.34^{d}	33.42^{a}	8.25^{ab}	13.74^{b}	1.26^{h}	510^{bc}	45.84^{c}	30.93^{e}	97.2^{e}	1.35^{abcd}
WsBC	300	5.44^{j}	0.7^{g}	6.84^{e}	0.03^{f}	9.11^{g}	1.9^{hi}	10.14^{b}	0.27^{kl}	100^{h}	14.36^{i}	35^{cd}	18.16^{i}	1.14^{bcd}
	400	4.58^{k}	0.59^{h}	4.88^{g}	0.07^{ef}	8.41^{gh}	1.86^{hi}	10.4^{b}	0.29^{k}	190^{g}	11.89^{j}	9.91^{jkl}	13.3^{jk}	1.1^{bcd}
	500	2.49^{m}	0.12^{j}	3.72^{h}	0.04^{f}	6.71^{hi}	0.85^{j}	9.01^{b}	0.24^{klm}	80^{hij}	11.21^{j}	9.84^{jkl}	11.09^{kl}	1.08^{bcd}
	600	2.13^{n}	0.1^{j}	3.21^{i}	0.02^{f}	5.26^{i}	0.44^{j}	8.64^{b}	0.18^{ml}	60^{ij}	9.96^{j}	9.63^{jkl}	9.84^{l}	1.06^{bcd}

[a] Means with different letters in the same column are significantly different (P≤ 0.05) by DMRT.

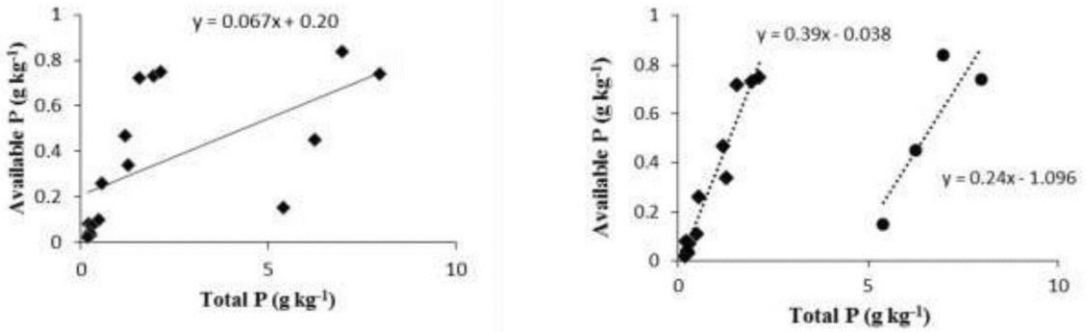

Figure 5. Correlation between total and available P concentration of TwBC, WhBC, WsBC and ApBC in four pyrolysis temperatures (left) and after separating TwBC data (y= 0.24x-1.096) from the rest (right).

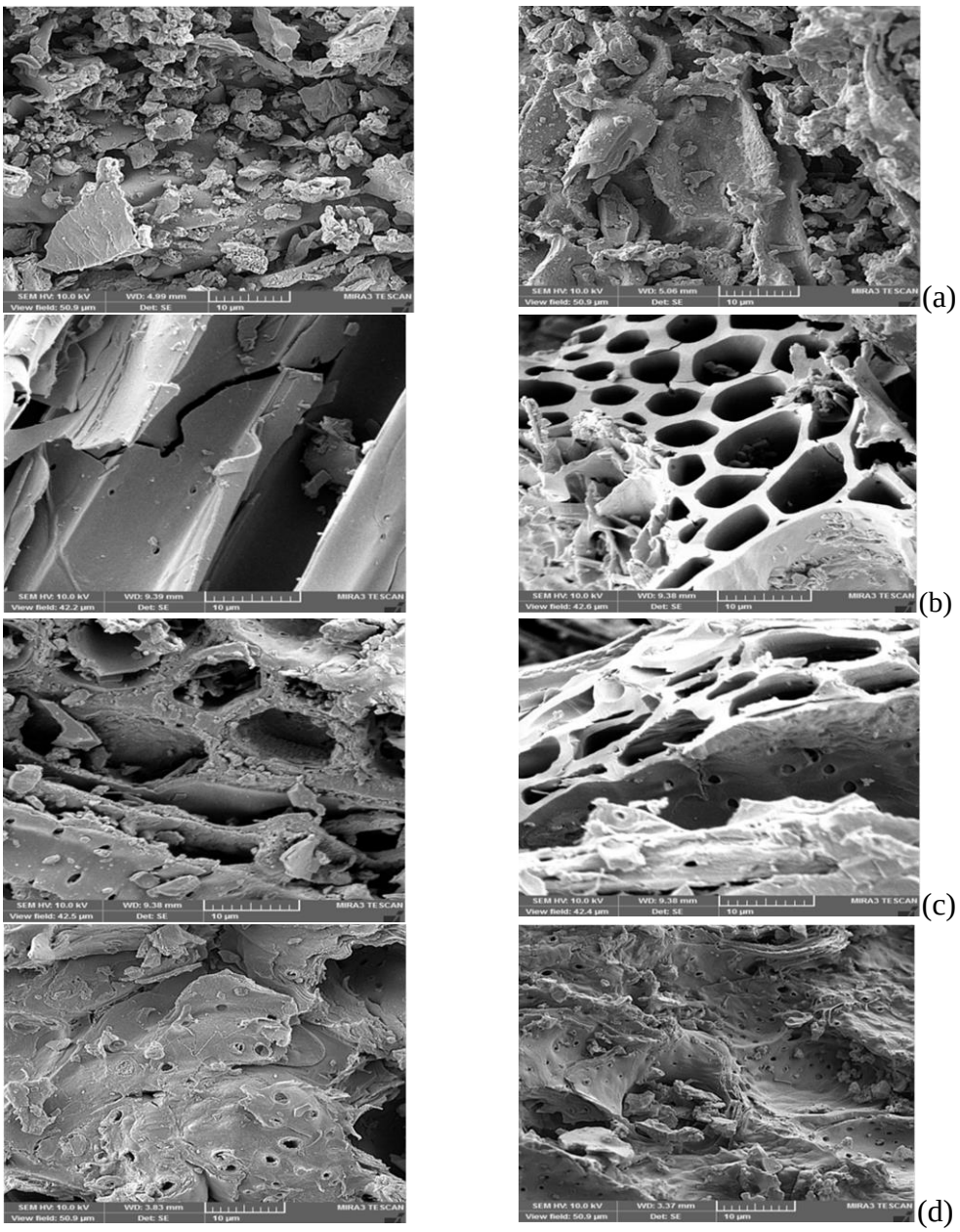

Figure 7. Scanning Electron Microscopy (SEM) micrographs (2500X magnification) of TwBC (a), WhBC (b), ApBC (c) and WsBC (d) biochars pyrolyzed at 300 (Left) and 600˚C (right), respectively.

Table 3. Specific surface area and pore size diameter for biochars produced at 300 and 600˚C.

Feedstock	Surface Area (m^2 g^{-1})		Pore size diameter (nm)	
	300˚C	600˚C	300˚C	600˚C
TwBC	5.40	70.83	5.97	3.05
WhBC	18.72	98.72	4.59	2.34
ApBC	1.93	147.66	9.35	2.91
WsBC	4.44	335.43	5.47	2.92

[DOR: 20.1001.1.16807073.2020.22.2.21.9]

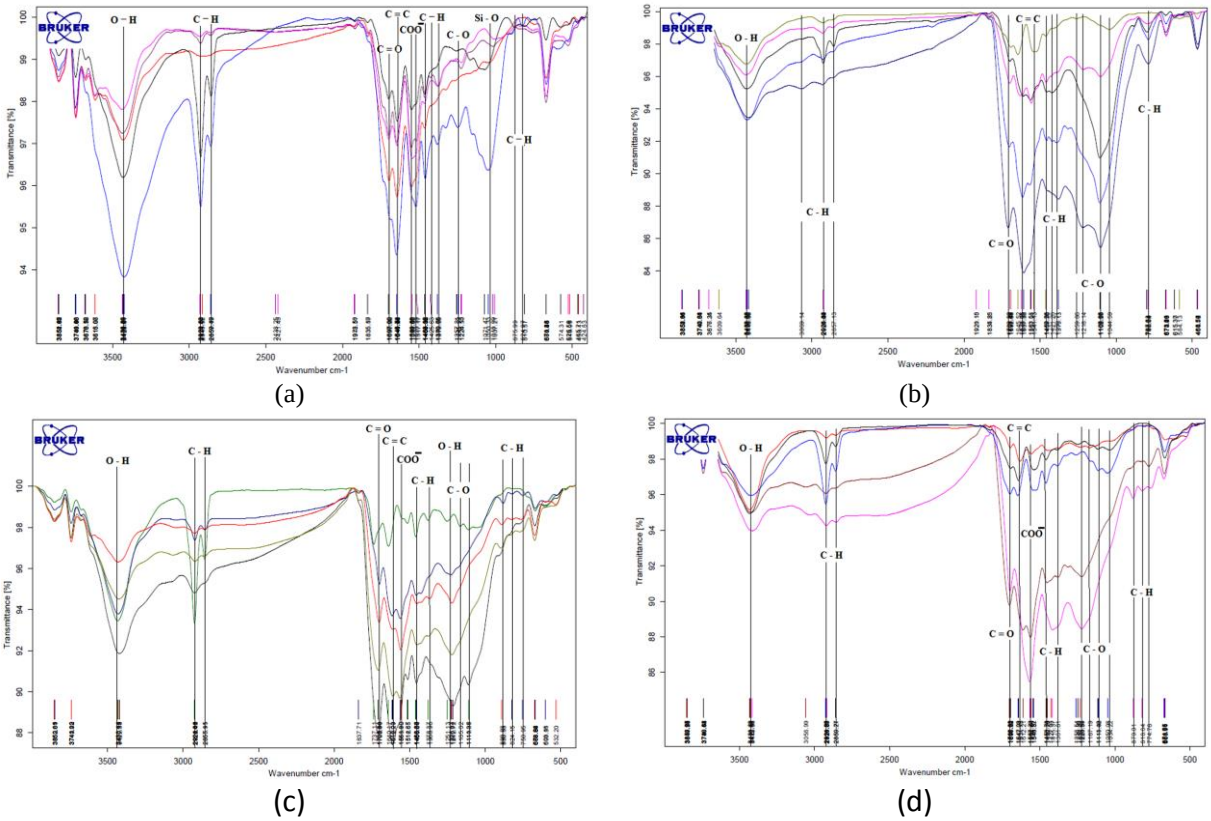

Figure 8. Fourier Transfer infra-red spectra (FT-IR) of TwBC (a), WhBC (b), ApBC (c) and WsBC (d), lines represented Feedstocks at 25˚C (blue) and biochars pyrolyzed at 300 (black), 400 (brown), 500 (pink) and 600˚C (red), respectively.

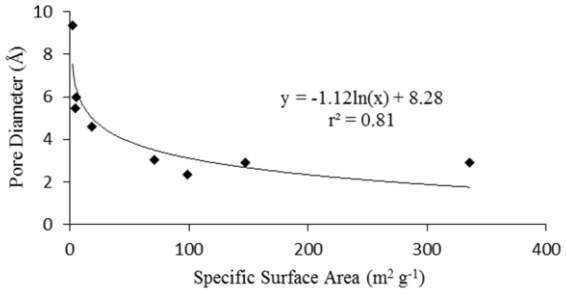

Figure 9. Relationships between the pore diameter and specific surface area for the produced biochars.

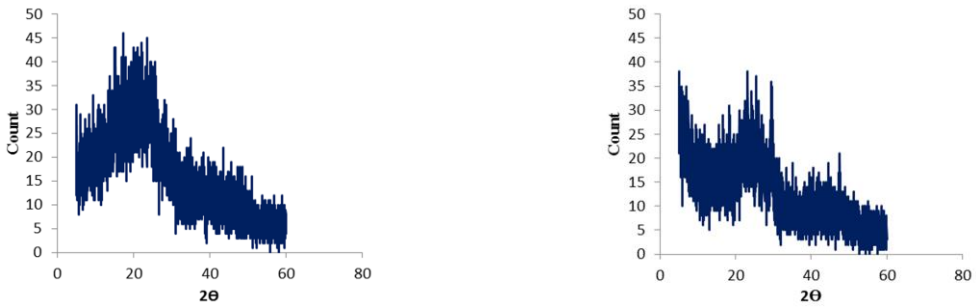

Figure 10. XRD patterns for TwBC at 300 (left) and 600˚C (right).

[DOR: 20.1001.1.16807073.2020.22.2.21.9]

elements, but linear correlation coefficient varied for K^+ (r= 0.97, P≤ 0.01), Ca^{2+} (r= 0.86, P≤ 0.01) and Mg^{2+} (r= 0.86, ns). The relationship between available and total concentration of Mg was non-linear and indicated that more available Mg (extracted by standardized 1M HCl solution) could be released from the total sources between 1 and 5 g kg^{-1} (Figure 6), and outside this range, total Mg has less effect on Mg availability.The specific surface area and pore size diameter values are given at Table 4. The highest amount of surface area was for WsBC at 600˚C, approximately 9-fold compared to 300˚C. More pores and long channels appeared in WhBC (Pituello *et al*., 2015), and in WsBC the large number of micropores became visible at a higher temperature. Relation between pore diameter and specific surface area for biochars is illustrated in Figure 9. It seems that without considering feedstock and pyrolysis temperature, the relation between pore diameter and specific surface area is in inverse logarithmic form.

Also, the surface area at 600˚C was markedly more than biochars produced at 300˚C, because of extinguishing volatile organic materials from feedstock structure that led to more void space on biochars (Lehman and Joseph, 2009). However, at the temperatures more than 700˚C, the micropores breakdown and total surface area declines (Chun *et al*., 2004). Because of the amorphous carbon and collapsed crystalline structure, XRD patterns were not clear to identify (Figure 10).

CONCLUSIONS

This study showed the structural and physicochemical dependency of biochars on nature of feedstock and pyrolysis temperature. By increments in pyrolysis temperature, the total and available concentration of elements in the produced biochars increased, except at walnut shell derived biochar. Strong positive linear relationships exist between available and total concentration of P, K, Ca in biochars, except Mg that showed nonlinear relation. The surface area of biochars increased by pyrolysis temperature but it was higher in woody materials than plant feedstock. Mean pore diameter decreased gradually, while surface area increased. These results of the chemical composition, structural properties, and surface bounding compounds suggest that biochars produced at 300 and 400˚C could be useful for calcareous soils because of low pH, low EC and high mass yield. Future characterization efforts could combine information of elemental contents and functional groups. Also, further research is recommended on the biochar effects on nutrients availability in calcareous soils.

ACKNOWLEDGEMENTS

This project is supported by a research grant of the University of Tabriz number (810). The authors thanks the University of Tabriz.

REFERENCES

1. Amonette, J. E. and Joseph, S. 2009. Characteristic of Biochar: Microchemical Properties. In: "*Biochar for Environmental Management Science and Technology"*, (Eds.): Lehmann J., and Joseph, S. Earthscan, London, PP. 33–43.
2. Antal Jr., M. J. and Gronli, M. 2003. The Art, Science, and Technology of Charcoal Production. *Ind. Eng. Chem. Res.*, **42:** 1619-1640.
3. ASTM. 2007. *D1762-84: Standard Methods for Chemical Analysis of Wool Charcoal.* American Society for Testing and Materials International, West Conshohocken, PA, USA.
4. Banitalebi, G., Mosaddeghi, M. R. and Shariatmadari, H. 2019. Feasibility of Agricultural Residues and Their Biochars for Plant Growing Media: Physical and Hydraulic Properties. *Waste Manag*., **87:** 577-589.

[DOR: 20.1001.1.16807073.2020.22.2.21.9]

5. Beesley, L., Moreno-Jiménez, E., Gomez-Eyles, J. L., Harris, E., Robinson, B. and Sizmur, T. 2011. A Review of Biochars Potential Role in the Remediation, Revegetation and Restoration of Contaminated Soils. *Environ. Pollut.*, **159:** 3269–3282.
6. Bera, T., Collins, H. P. Alva, A. K., Purakayastha, T. J. and Patra, A. K. 2016. Biochar and Manure Effluent Effects on Soil Biochemical Properties under Corn Production, *Appl. Soil Ecol*., **107:** 360–367.
7. Bera, T., Purakayastha, T. J., Patra, A. K. and Datta. S. C. 2018. Comparative Analysis of Physicochemical, Nutrient, and Spectral Properties of Agricultural Residue Biochars as Influenced by Pyrolysis Temperatures. *J. Mater. Cycles Waste Manag.*, **20:** 1115–1127.
8. Bera, T., Vardanyan, L., Inglett, K. S., Reddy, K. R., O'Connor, G. A., Erickson, J. E. and Wilkie. A. C. 2019. Influence of Select Bioenergy By-Products on Soil Carbon and Microbial Activity: A Laboratory Study. *Sci. Total. Environ.*, **653:** 1354 -1363.
9. Cantrell, K., Hunt, P. G., Uchimiya, M., Novak, J. M. and Ro, K. S. 2012. Impact of Pyrolysis Temperature and Manure Source on Physicochemical Characteristics of Biochar. *Bioresour. Technol.*, **107:** 419-428.
10. Chun, Y., Sheng, G. Y., Chiou, C. T. and Xing, B. S. 2004. Compositions and Sorptive Properties of Crop Residue-Derived Chars. *Enviro. Sci. Technol.*, **38:** 4649–4655.
11. Claoston, N. A., Samsuri, M. H. and Husni, A. 2014. Effects of Pyrolysis Temperature on the Physicochemical Properties of Empty Fruit Bunch and Rice Husk Biochars. *Waste Manag. Res.*, **32(4):** 331-339.
12. Enders, A., Hanley, K., Whitman, T., Joseph, S. and Lehmann, J. 2012. Characterization of Biochars to Evaluate Recalcitrance and Agronomic Performance. *Bioresour. Technol.*, **114:** 644–653.
13. Fang, Q., Chen, B., Lin, Y. and Guan, Y. 2014. Aromatic and Hydrophobic Surfaces of Wood-Derived Biochar Enhance Perchlorate Adsorption *via* Hydrogen Bonding to Oxygen Containing Organic Groups. *Environ. Sci. Technol.*, **48:** 279−288.
14. Ghani, W., Mohd, A., da Silva, G., Bachmann, R., Taufiq-Yap, Y., Rashid, U. and Al-Muhtaseb, A. 2013. Biochar Production from Waste Rubber-Wood Sawdust and Its Potential Use in C Sequestration: Chemical and Physical Characterization. *Ind. Crop Prod.*, **44:** 18-24.
15. Guo, J. and Chen, B. 2014, Insights on the Molecular Mechanism for the Recalcitrance of Biochar: Interactive Effects of Carbon and Silicon Components. *Environ. Sci. Technol.*, **48:** 9103–9101.
16. IBI. 2015. Standardized Product Definition and Product Testing Guidelines for Biochar that Is Used in Soil. Version 2.1. *International Biochar Initiative*, 61 PP. http://www.biochar-international.org/sites/default/files/IBI-Biochar_Standards_V2.0_final.pdf>.
17. Jia, Y., Shi, S., Liu, J., Su, S., Liang, Q., Zeng, X. and Li, T. 2018. Study of the Effect of Pyrolysis Temperature on the Cd2+ Adsorption Characteristics of Biochar. *Appl. Sci.*, **8(1019):** 1-14.
18. Jindo, K., Mizumoto, H., Sawada, Y., Sanchez-Monedero M. A. and Sonoki, T. 2014. Physical and Chemical Characterization of Biochars Derived from Different Agricultural Residues. *Biogeosciences*, **11:** 6613-6621.
19. Joseph, S., Downie, A., Munroe, P. and Crosky, A. 2007. Biochar for Carbon Sequestration, Reduction of Greenhouse Gas Emissions and Enhancement of Soil Fertility: A Review of the Materials Science. *Proceeding of the Australian Combustion Symposium*: *Emissions* and *Enhancement* of *Soil Fertility*, PP. 130-133.
20. Karimi Alavijeh, M. and Yaghmaei, S. 2016. Biochemical Production of Bioenergy from Agricultural Crops and Residue in Iran. *Waste Manag.*, **52:** 375-394.
21. Kim, K. H., Kim, J. Y., Cho, T. S. and Choi, J. W. 2012. Influence of Pyrolysis Temperature on Physicochemical Properties of Biochar Obtained from the Fast Pyrolysis of Pitch Pine. *Bioresour. Technol*., **118:** 158-162.

[DOR: 20.1001.1.16807073.2020.22.2.21.9]

22. Lee, Y., Park, J., Ryu, C., Gang, K. S., Yang, W., Park, Y-K., Jung, J. and Hyun, S. 2013. Comparison of Biochar Properties from Biomass Residues Produced by Slow Pyrolysis at 500°C. *Bioresour. Technol.*, **148:** 196–201.
23. Lehmann, J. and Joseph, S. 2009. Biochar for Environmental Management: Science and Technology. Earthscan, London, 448 PP.
24. Li, M. Liu, Q. Guo, L. Zhang, Y. Lou, Z. Wang, Y. and Qian, G. 2013. Cu(II) Removal from Aqueous Solution by *Spartina alterniflora* Derived Biochar. *Bioresour. Technol.*, **141:** 83–88.
25. Liu, Z., and Han, G. 2015. Production of Solid Fuel Biochar from Waste Biomass by Low Temperature Pyrolysis. *Fuel*, **158:** 159-165.
26. Liu, Z., Niu, W., Chu, H., Zhou, T. and Niu, Z. 2018. Effect of the Carbonization Temperature on the Properties of Biochar Produced from the Pyrolysis of Crop Residues. *Bioresour*., **13(2):** 3429-3446.
27. Luo, L., Xu, C., Chen, Z. and Zhang, S. 2015. Properties of Biomass-Derived Biochars: Combined Effects of Operating Conditions and Biomass Types. *Bioresour. Technol.*, **192:** 83-89.
28. Mohan, D., Pittman, C. U. and Steele, P. H. 2006. Pyrolysis of Wood/Biomass for Bio Oil: A Critical Review. *Energ. Fuels*, **20:** 848-889.
29. Mukome, F. N. D., Zhang, X., Silva, L. C. R., Six, J. and Parikh, S. J. 2013. Use of ChemIcal and Physical Characteristics to Investigate Trends in Biochar Feedstocks. *J. Agric. Food Chem.,* **61:** 2196–2204.
30. Nanda, S., Mohanty, P., Pant, K. K., Naik, S., Kozinski, J. A. and Dalai, A. K. 2013. Characterization of North American Lignocellulosic Biomass and Biochars in Terms of Their Candidacy for Alternate Renewable Fuels. *BioEnerg. Res*., **6:** 663–677.
31. O'Connor, D., Peng, T., Zhang, J., Tsang, D. C. W., Alessi, D. S., Shen, Z., Bolan N. S., and Hou, D. 2018. Biochar Application for the Remediation of Heavy Metal Polluted Land: A Review of *in Situ* Field Trials. *Sci. Total Environ.*, **619–620:** 815–826.
32. Pituello, C., Francioso, O., Simonetti, G., Pisi, A., Torreggiani, A., Berti, A. and Morari, F. 2015. Characterization of Chemical–Physical, Structural and Morphological Properties of Biochars from Biowastes Produced at Different Temperatures. *J. Soils Sediments*, **15:** 792–804.
33. Reeves, J. B., McCarty, G. W., Rutherford, D. W. and Wershaw, R. L. 2007. Near Infrared Spectroscopic Examination of Charred Pine Wood, Bark, Cellulose and Lignin: Implications for the Quantitative Determination of Charcoal in Soils. *J. Near Infrared Spec*., **15:** 307-315.
34. Rens, H., Bera, T. and. Alva, A. K. 2018. Effects of Biochar and Biosolid on Adsorption of Nitrogen, Phosphorus, and Potassium in Two Soils. *Water Air Soil Pollut*., **229(8)**:281.
35. Rostamian, R., Heidarpour, M., Mousavi, S. F. and Afyuni, M. 2015. Characterization and Sodium Sorption Capacity of Biochar and Activated Carbon Prepared from Rice Husk. *J. Agr. Sci. Tech.*, **17:** 1057-1069.
36. Sandhua, S. S., Ussiri, D. A. N., Kumar, S., Chintala, R., Papiernik, S. K., Malo, D. D. and Schumacher, T. E. 2017. Analyzing the Impacts of Three Types of Biochar on Soil Carbon Fractions and Physiochemical Properties in a Corn-Soybean Rotation. *Chemosphere*, **184:** 473-481.
37. Shen Z., Hou, D., Jin, F., Shi, J., Fan, X., Tsang, D. C. W. and Alessi, D. S. 2019. Effect of Production Temperature on Lead Removal Mechanisms by Rice Straw Biochars. *Sci. Total Environ*., **655:** 751–758.
38. Singh, B., Camps-Arbestain, M. and Lehmann, J. 2017. *Biochar: A Guide to Analytical Methods*. CSIRO Publishing, Australia, 310 PP.
39. Singh, B., Singh, B. P. and Cowie, A. L. 2010. Characterisation and Evaluation of Biochars for Their Application as a Soil Amendment. *Aust. J. Soil Res*., **48:** 516-525.
40. Sun X., Shan, R., Li, X., Pan, J., Liu, X., Deng, R. and Song, J. 2017. Characterization of 60 Types of Chinese Biomass Waste and Resultant Biochars in Terms of Their Candidacy for Soil Application. *Bioenergy*, **9:** 1423-1435.

[DOR: 20.1001.1.16807073.2020.22.2.21.9]

41. Thangalazhy-Gopakumar, S., Adhikari, S., Ravindran, H., Gupta, R. B., Fasina, O., Tu, M. and Fernando, S. D. 2010. Physiochemical Properties of Bio-Oil Produced at Various Temperatures from Pine Wood Using an Auger Reactor. *Bioresour. Technol.*, **101(21):** 8389-8395.
42. Tsai, W. T., Liu, S. L., Chen, H. R., Chang, Y. M. and Tsai, Y. L. 2012. Textural and Chemical Properties of Swine-Manure-Derived Biochar Pertinent to Its Potential Use as a Soil Amendment. *Chemosphere*, **89(2):** 198-203.
43. Usman, A.R.A., Abduljabbar, A., Vithanage, M., Ok, Y. S., Ahmad, M., Ahmad, M., Elfaki, J., Abdulazeem, S. S. and Al-Wabel, M. I. 2015. Biochar Production from Date Palm Waste: Charring Temperature Induced Changes in Composition and Surface Chemistry. *J. Anal. Appl. Pyrolysis*, **115:** 392–400.
44. Westerman, R. L. 1990. Soil Testing and Plant Analysis. 3. In*: "The Soil Science Society of America Book Series".* Third Edition, Soil Science Society of America, Inc., Madison, Wisconsin, USA, 784 PP.
45. Wu, W., Yang, M., Feng, Q., McGrouther, K., Wang, H., Lu, H. and Chen, Y. 2012. Chemical Characterization of Rice Straw-Derived Biochar for Soil Amendment. *Biomass Bioenerg.*, **47:** 268–276.
46. Yang, X., Wang, H., Strong, P.J., Xu, S., Liu, S., Lu, K., Sheng, K., Guo, J., Che, L., He, L., Ok, Y.S., Yuan, G., Shen, Y. and Chen, X. 2017. Thermal Properties of Biochars Derived from Waste Biomass Generated by Agricultural and Forestry Sectors. *Energies*, **10(469).** doi:10.3390/en10040469.
47. Yu, H., Zou, W., Chen, J., Hao Chen, H., Yu, Z., Huang, J., Tang, H., Wei, X. and Gao, B. 2019. Biochar Amendment Improves Crop Production in Problem Soils: A Review. *J. Environ. Manag.*, **232:** 8-21.
48. Zhang, Z., Zhu, Z., Shen, B. and Liu, L. 2019. Insights into Biochar and Hydrochar Production and Applications: A Review. *Energy*, **171:** 581-598.

تاثیر دمای پیرولیز و منبع زیست توده بر ویژگی‌های فیزیکو شیمیایی بیوچار

ع. ریحانی تبار، ا. فرهادی، ح. رمضانزاده، و ش. اوستان

چکیده

یکی از رهیافت‌های رایج غلبه بر مشکل دفع ضایعات آلی حاصل از فعالیتهای کشاورزی تبدیل آنها به بیوچار است. اما نقش نوع پس ماند و دمای پیرولیز بر ویژگیهای فیزیکوشیمیایی بیوچار هنوز به خوبی درک نشده است. در این مطالعه نمونه های بیوچار از بیوماس های اولیه مختلف همانند تفاله چای، چوب درخت سیب، کاه گندم و پوسته گردو در دماهای ۳۰۰و۴۰۰و۵۰۰و۶۰۰ درجه سلسیوس با زمان ماندگاری یک ساعت تولید شدند. نتایج نشان داد که با افزایش دمای پیرولیز، عملکرد بیوچار کاهش معناداری یافت. بیشینه و کمینه عملکرد در بیوچار حاصل از پوسته گردو در دمای ۳۰۰ درجه و چوب درخت سیب در دمای ۶۰۰ به ترتیب برابر ۶۹/۲ و ۱۹/۹ درصد حاصل شد. پ هاش بیوچارهای تولید شده دارای دامنه ۵.۳ تا ۹.۷ بودند و مقدار پ هاش و محتوای خاکستر در تمام نمونه ها با افزایش دمای پیرولیز به استسنای پوست گردو افزایش یافت. غلظت کل عناصر فسفر، کلسیم، پتاسیم، سدیم، آهن، روی، مس و منگنز و غلظت قابل جذب پتاسیم، کلسیم، منیزیم و فسفر با افزایش دمای پیرولیز به

[DOR: 20.1001.1.16807073.2020.22.2.21.9]

استسنای بیوچار حاصل از پوسته گردو افزایش یافت. بر طبق نتایج آنالیز CHN، با افزایش دما غلظت کل کربن افزایش و نیتروژن و هیدروژن کاهش یافتند. همچنین پ هاش تا ۷۲ ساعت کاهش و سپس تقریبا به شرایط پایدار رسید. رابطه بین پ هاش و مقدار کربنات کلسیم نزدیک و خطی بود. طیف سنجی FT-IR نمونه ها نشان داد که کربن آروماتیک با افزایش دما افزایش یافت. همچنین با افزایش دمای پیرولیز متوسط قطر منافذ کاهش اما حجم میکروپورها افزایش یافت که منجر به افزایش سطح ویژه نمونه های بیوچار شد. نتایج این مطالعه نشان می دهد که بیوچارهای تولیدی در دمای ۳۰۰ و ۴۰۰ درجه سلسیوس به دلیل pH و EC پایین و عملکرد بالا ممکن است از پتانسیل کودی در خاک‌های آهکی برخوردار باشند.

[DOR: 20.1001.1.16807073.2020.22.2.21.9]